SPECIAL FEATURE

Modeling quantum fluid dynamics at nonzero temperatures

Natalia G. Berloff[a,b,1], Marc Brachet[c], and Nick P. Proukakis[d]

[a]Department of Applied Mathematics and Theoretical Physics, University of Cambridge, Cambridge CB3 0WA, United Kingdom; [b]Cambridge-Skoltech Quantum Fluids Laboratory, Skolkovo Institute of Science and Technology ul. Novaya, Skolkovo 143025, Russian Federation; [c]Centre National de la Recherche Scientifique, Laboratoire de Physique Statistique, Université Pierre-et-Marie-Curie Paris 06, Université Paris Diderot, Ecole Normale Supérieure, 75231 Paris Cedex 05, France; and [d]Joint Quantum Centre (JQC) Durham–Newcastle, School of Mathematics and Statistics, Newcastle University, Newcastle upon Tyne NE1 7RU, United Kingdom

Edited by Katepalli R. Sreenivasan, New York University, New York, NY, and approved December 13, 2013 (received for review July 15, 2013)

The detailed understanding of the intricate dynamics of quantum fluids, in particular in the rapidly growing subfield of quantum turbulence which elucidates the evolution of a vortex tangle in a superfluid, requires an in-depth understanding of the role of finite temperature in such systems. The Landau two-fluid model is the most successful hydrodynamical theory of superfluid helium, but by the nature of the scale separations it cannot give an adequate description of the processes involving vortex dynamics and interactions. In our contribution we introduce a framework based on a nonlinear classical-field equation that is mathematically identical to the Landau model and provides a mechanism for severing and coalescence of vortex lines, so that the questions related to the behavior of quantized vortices can be addressed self-consistently. The correct equation of state as well as nonlocality of interactions that leads to the existence of the roton minimum can also be introduced in such description. We review and apply the ideas developed for finite-temperature description of weakly interacting Bose gases as possible extensions and numerical refinements of the proposed method. We apply this method to elucidate the behavior of the vortices during expansion and contraction following the change in applied pressure. We show that at low temperatures, during the contraction of the vortex core as the negative pressure grows back to positive values, the vortex line density grows through a mechanism of vortex multiplication. This mechanism is suppressed at high temperatures.

superfluidity | ZNG theory | (truncated) Gross–Pitaevskii equation | stochastic Ginzburg–Landau equation | quantum Boltzmann equation

In this article we propose a framework for modeling the Landau two-fluid dynamics in superfluids with the intention of laying the groundwork for the study of the effects of interconnecting mixture of superfluid and normal fluid components on vortices and quantum turbulence in superfluid helium.

We are concerned here with systems that are described by an order parameter ψ, a classical matter field characterizing the collective behavior of the ensemble of particles. The quantum mechanical interpretation of the order parameter gives the number density n and velocity $\mathbf{v}$ via the Madelung transformation $\psi=\sqrt{n}\exp[i\phi]$, $\mathbf{v}=\hbar/m\nabla\phi$. The single-valuedness of ψ leads to a key aspect of a superfluid: quantization of circulation $\Gamma\equiv\oint\mathbf{v}\cdot d\mathbf{l}=jh/m$, where h is Planck's constant, m is atomic mass, j is an integer, and the integral is taken for any closed contour moving with the fluid. The presence of vortices can lead both to organized arrays known as vortex lattices (1), and to random arrays of tangles of vortices (2). Unlike classical systems, characterized by continuous vorticity, quantum systems exhibit quantized circulation; here turbulence can manifest itself in a number of ways, summarized, e.g., in ref. 3.

Quantum turbulence studies are concerned with the relaxation kinetics and dynamics of a vortex tangle, with some key issues in this context relating to the universal features of steady-state forced 3D superfluid turbulence (3–13), the emergence of an inverse cascade in 2D systems (14–16), and the precise mechanisms and dynamics of the decay of turbulence (17–19). Whereas large-scale features of classical and quantum turbulence are similar [e.g., Kolmogorov spectrum (9–13)], features sensitive to the vortex core structure arising at lengthscales smaller than the average intervortex spacing [e.g., velocity statistics (20–22) and pressure (23)] show starkly different behavior—see, e.g., the recent reviews (24, 25). In addition to liquid helium (2, 26), there has been some recent interest in the observation of turbulence in smaller inhomogeneous confined weakly interacting gases (27, 28); such systems offer unprecedented experimental control and ab initio modeling (29), with their finite size, high compressibility, and lower disparity between intervortex distances and core sizes (compared with superfluid helium) leading to the probing of a very different turbulent regime (30).

Despite the large body of research on superfluid turbulence, numerous questions remain that can only be answered by proper modeling of superfluid and normal fluid behavior and interactions including processes associated with quantized vortices. The aim of this article is to introduce a framework for achieving this task while making use of existing methods for modeling the thermal component and to apply one of these methods to an important research question in liquid helium experiments (31, 32). We do not thus attempt to give an overview of existing results in the context of superfluid turbulence—discussed in detail in recent reviews (3–5, 22, 33, 34)—but instead highlight the key predictions of such methods in describing single-vortex dynamics, as a first step toward a "bottom-up" approach to superfluid turbulence.

Brief Historical Overview

The first successful theory of superfluid helium was proposed by Landau shortly after the discovery of superfluidity (35). Using purely classical arguments and the principle of Galilean invariance, Landau modeled superfluid helium as an interpenetrating mixture of a superfluid and normal fluid components (denoted, respectively, by subscripts s and n). Landau's formulation of the two-fluid model was in the form of conservation laws for the total density ρ, the specific entropy s, the total momentum $(\rho_n\mathbf{v}_n+\rho_s\mathbf{v}_s)$, and the superfluid velocity $\mathbf{v}_s$ (see *SI Text* for an explicit formulation and ref. 29 for discussions). In this context, the normal fluid represents a sea of elementary excitations that ride on the superfluid. Below the transition temperature T_λ, a superfluid state emerges; with further decrease in temperature the density of the normal component decreases and the density of superfluid increases until at $T=0$ the normal component disappears. In the context of quantum turbulence, the normal fluid determines the properties of the turbulent state for relatively high temperatures, with superfluid vorticity following the normal fluid vorticity distribution. Close to zero temperature the role of the components is reversed, with the

Author contributions: N.G.B. designed research; N.G.B. performed research; M.B. and N.P.P. contributed new analytic tools; and N.G.B., M.B., and N.P.P. wrote the paper.

The authors declare no conflict of interest.

This article is a PNAS Direct Submission.

[1]To whom correspondence should be addressed. E-mail: N.G.Berloff@damtp.cam.ac.uk.

This article contains supporting information online at www.pnas.org/lookup/suppl/doi:10.1073/pnas.1312549111/-/DCSupplemental.

turbulence in the superfluid determining the turbulence of the normal component.

The Landau two-fluid model predated the discovery of quantized vorticity. The tension between vortices and mutual friction between vortices and normal fluid were added phenomenologically to the two-fluid model by Hall et al. (36) and Bekarevich and Khalatnikov (37). The resulting Hall–Vinen–Bekarevich–Khalatnikov (HVBK) theory scored some success in cases of high density of superfluid vortex lines of known orientation, for instance, in explaining the instability of Taylor–Couette flow (38).

HVBK cannot be applied when the dynamics and relaxation of the vortex tangle are important, as it treats superfluid vorticity as continuum and therefore excludes the processes leading to vortex reconnections that drive the vortex tangle relaxation. To model the evolution of the vortex tangle another classical approach was introduced (39–41), which is now the most widely accepted method in studying quantum turbulence. In this approach superfluid vortices are modeled as classical Eulerian vortices of zero cross-section with δ-function vorticity that move according to the Biot–Savart law

$$\mathbf{v}(\mathbf{x}) = \frac{\kappa}{4\pi}\int \frac{\mathbf{s}'\times(\mathbf{x}-\mathbf{s})\,d\xi}{|\mathbf{x}-\mathbf{s}|^3}, \qquad [1]$$

where $\mathbf{s}(\xi)$ is the vortex filament parameterized by arc length ξ, and $\mathbf{s}'(\xi)=d\mathbf{s}/d\xi$ is the unit tangent vector. The effect of the normal fluid is included phenomenologically by adding mutual friction coefficients α and α' to the equation of filament motion

$$\frac{d\mathbf{s}}{dt} = \mathbf{v}_s + \mathbf{v} + \alpha\mathbf{s}'\times(\mathbf{v}_n-\mathbf{v}_s-\mathbf{v}) - \alpha'\mathbf{s}'\times\left[\mathbf{s}'\times(\mathbf{v}_n-\mathbf{v}_s-\mathbf{v})\right], \qquad [2]$$

where $\mathbf{v}_n$ and $\mathbf{v}_s$ are ambient velocities of the normal and superfluid components. Its effect on the vortex filament is well illustrated by considering a vortex ring of radius R. At $T=0$, in the absence of the normal fluid and ambient superfluid, Eq. **2** with $\mathbf{v}$ given by Eq. **1** implies that the vortex moves maintaining its shape with a constant velocity $u(R)$, which within logarithmic accuracy is $u(R)=\hbar/(2mR)\ln(R/\xi)$, where ξ is the vortex core size. In the presence of the normal fluid there is a drag on the ring, forcing the radius of the ring to shrink at the rate given by $dR/dt=-\alpha u(R)$. Many aspects important to quantum turbulence are omitted in this framework. The dynamics of vortices in compressible fluids is quite different from that in incompressible fluids, in particular the effect of sound generation during reconnections and scattering sound waves is completely neglected. Also, the reconnections of vortices and the cutoff to salvage the divergence of the integral in Eq. **1** as $\mathbf{x}\to\mathbf{s}_0$, where $\mathbf{s}_0$ is the point on the vortex filament, have to be introduced phenomenologically.

In the next sections we introduce a framework for modeling the Landau two-fluid model that includes the interaction of vortices, consider various alternative frameworks to model nonequilibrium processes in quantum fluids, discuss some of their key predictions in the context of quantum vortex evolution, and finally apply one of these techniques to study the behavior of the vortex rings in a finite-temperature homogeneous system during expansion and contraction following the change in applied pressure.

Landau Two-Fluid Model for a One-Component Fluid

We start by writing an equation for the time evolution of the classical complex function ψ in the form of a generalized nonlinear Schrödinger equation (gNLSE)

$$i\hbar\frac{\partial\psi}{\partial t} = \left[E(i\nabla) + \int |\psi(\mathbf{x}')|^2 V(|\mathbf{x}-\mathbf{x}'|)d\mathbf{x}' + \mu\left(|\psi|^2\right)\right]\psi, \qquad [3]$$

where $V(|\mathbf{x}-\mathbf{x}'|)$ is a two-body interaction potential representing nonlocality of interactions; the intrinsic dispersion of elementary excitations is represented by $E(k)$, which for the quadratic dispersion becomes $E(k)=\hbar^2k^2/2m$, where m is the particle mass. The chemical potential μ is connected to pressure P via $d\mu(n)=(1/n)dP(n)$ and comes from the equation of state of the system. The small perturbations of the uniform number density $n_0=N/\mathcal{V}$, where N is the number of particles occupying the volume $\mathcal{V}$, satisfy the dispersion law

$$\omega^2 = \frac{\hbar^2}{4m^2}k^4 + c_0^2k^2 + (n_0/m)\tilde{V}(k)k^2, \qquad [4]$$

where $\tilde{V}(k)=\int V(r)\exp[-i\mathbf{k}\cdot\mathbf{r}]d\mathbf{r}$, and the speed of sound c_0 is set by $c_0^2=(1/m)\partial P/\partial n_0$. The pressure relates to the energy per particle by $P=n_0^2\partial(E/N)/\partial n_0$. Neglecting the nonlocality of interactions leads to the cubic or higher-order nonlinear Schrödinger equations (NLSEs). For the weakly interacting Bose gases the equation of state is known to be $E/N=V_0n_0/2$, leading to the cubic NLSE [in the context of dilute weakly interacting Bose gases also commonly referred to as the Gross–Pitaevskii equation (GPE) (42)],

$$i\hbar\frac{\partial\psi}{\partial t} = -\frac{\hbar^2}{2m}\nabla^2\psi + V_0|\psi|^2\psi. \qquad [5]$$

The higher-order NLSE results for denser fluids such as superfluid ^{4}He for which the equation of state is well approximated by the polynomial expansion

$$\frac{E}{N} = -\frac{V_0}{2}n_0 - \frac{V_1}{3}n_0^2 + \frac{V_2}{4}n_0^3, \qquad [6]$$

where $V_0=719K\mathring{A}^3k_B$, $V_1=3.63\times10^4K\mathring{A}^6k_B$ and $V_2=2.48\times10^6K\mathring{A}^9k_B$, are fixed to reproduce the properties of superfluid helium over a range of pressures (42). This leads to the higher-order NLSE

$$i\hbar\frac{\partial\psi}{\partial t} = \left[-\frac{\hbar^2}{2m}\nabla^2 - V_0|\psi|^2 - V_1|\psi|^4 + V_2|\psi|^6\right]\psi. \qquad [7]$$

This form of the equation has been used to study the instability of the vortices and cavitation at negative pressures and $T=0$ (43, 44) showing the quantitative agreement with experiments (32). The dispersion **4** for the cubic NLSE reproduces the Bogoliubov spectrum of the dilute weakly interacting gaseous atomic BECs quite well. Superfluid helium has a roton minimum of the dispersion curve that can be modeled by keeping the nonlocal interactions $V(r)$. The quantitatively correct dispersion curve in this case can be obtained for a range of potentials; for instance the Lennard-Jones potential with attractive interactions at short distances can be modeled by

$$V(|\mathbf{x}-\mathbf{x}'|) = V(r) = (b_1 + b_2r^2 + b_3r^4)\exp(-B^2r^2), \qquad [8]$$

with phenomenological parameters b_1, b_2, b_3, and B chosen so that the dispersion curve **4** gives a good fit to the phonon, maxon, and roton parts of the superfluid helium spectrum (45, 46). Such a nonlocal model has been used to elucidate the difference between roton creation and vortex nucleation in superfluids (47), while treating ψ as the wave function of the condensate. In this context the gNLSE is at best only a phenomenological model of superfluid helium because in helium there always exists a strong coupling of highly occupied modes with modes of low occupation due to strong interactions. In what follows we instead interpret the gNLSE as a mathematical model that brings about the Landau two-fluid model and treats vortices self-consistently, so the complex function ψ is no longer directly associated with the condensate.

The Madelung transformation converts real and imaginary parts of Eq. **3** into the hydrodynamic equations for the conservation of mass

$$\partial n/\partial t + \nabla \cdot (n\mathbf{v}) = 0, \quad [9]$$

and the integrated form of the equation of motion (Newton's law for continuous fluid elements in Eulerian description)

$$m\partial \mathbf{v}/\partial t + m(\mathbf{v}\cdot\nabla)\mathbf{v} = -\nabla\mu_0(n), \quad [10]$$

where the chemical potential μ_0 includes the nonlocal term and the density functional (quantum pressure) coming from the Laplacian

$$\mu_0(n) = \mu(n) + \int n(\mathbf{x}')V(|\mathbf{x}-\mathbf{x}'|)d\mathbf{x}' - \frac{\hbar^2}{2m^2}\frac{\nabla^2\sqrt{n}}{\sqrt{n}}. \quad [11]$$

Putterman and Roberts (48) have shown that starting from a general framework of Eqs. **9** and **10** and using a scale-separation argument, it is possible to derive a set of kinetic equations that describe the dynamics of thermal noncondensed excitations and their interactions with the condensate. In the collision-dominated regime they recovered the Landau two-fluid model that represents the evolution of the normal fluid component and superfluid components. This separation is possible as the solution of Eqs. **9** and **10** and therefore of Eq. **3** contains a long-wavelength slow background associated with the superfluid component and short-wavelength fast excitations associated with the normal component (thermal cloud). These two types of motion should be coupled by nonlinearities of Eq. **3**, but in the reversible limit this coupling will vanish and the system possesses conserved quantities leading to extra velocity and density fields. Such separation is achieved by expanding n (and similarly $\mathbf{v}$) in terms of slowly varying backgrounds, n_c, and high-frequency waves, n_i

$$n(\mathbf{x},t) = n_c(\delta\mathbf{x},\delta t) + \epsilon[n_1(\delta\mathbf{x},\delta t) + \delta n_2(\delta\mathbf{x},\delta t)]\exp(i\theta), \quad [12]$$

where θ satisfies the differential form $d\theta = \mathbf{k}\cdot d\mathbf{x} - \omega dt$ and the relationship between the small parameters δ and ϵ determines the distinction between collisionless ($\epsilon^2 \ll \delta \ll \epsilon \ll 1$) and collision-dominating regimes ($\delta \ll \epsilon^4 \ll 1$). In the collisionless regime the Vlasov wave equation emerges, describing the evolution of Bogoliubov quasiparticles. The collision integrals and the kinetic Boltzmann equations in the collision-dominated regime can be derived in a rigorous way using the matched asymptotics (49). The wave kinetics in this case describes three-wave and four-wave interactions with the resonance conditions arising from momentum and energy conservations of Eq. **3**. They are analogous to the Zaremba, Nikuni, and Griffin kinetic equations (see subsequent section *Coupled Kinetic Equations: The Zaremba, Nikuni, and Griffin Model*), but without spontaneous scattering present.

Because the Landau two-fluid dynamics can be derived from a one-component classical nonlinear field described by a rather general form of nonlinearity, the one-component model can be used to model superfluids at finite temperature. The cubic NLSE has been argued to give an accurate microscopic description of the formation of a Bose–Einstein condensate (BEC) from the strongly degenerate gas of weakly interacting bosons (50–53) and the stages of that formation from a strongly nonequilibrium initial condition were elucidated (54). It has also been used to describe the equilibrium fluctuations of the condensate and highly occupied noncondensate modes (55, 56). By now the method of using a cubic NLSE to model finite-temperature or quantum (49) effects in Bose gases has become relatively common, with slightly different viewpoints portrayed, e.g., in refs. 29, 57, 58; see also the section below *Truncated Equations of Nonlinear Classical Fields*.

In the context of modeling the finite-temperature superfluid ^{4}He, the phenomenological model of Eq. **3** has not been used. For the system to evolve as an ensemble of classical fields with corresponding classical-field action, the occupation numbers must be large and somewhat uncertain (59), which is only possible in a weakly interacting system. In a strongly interacting system, such as superfluid helium, there are always small occupation numbers that are coupled with high occupation numbers and the behavior of the quantum system cannot be accurately described by the classical-field approximation. The proposed framework of using Eq. **3** thus arises not as an accurate description of a quantum system, but as a mathematical analog of the Landau two-fluid model.

In homogeneous systems the separation of superfluid and normal fluid components is rather straightforward to implement numerically. We consider the evolution of the field

$$\psi(\mathbf{x},t) = \sum_{\mathbf{k}} a_{\mathbf{k}}\exp(i\mathbf{k}\cdot\mathbf{x}), \quad [13]$$

where the complex Fourier amplitudes $a_{\mathbf{k}}$ define the occupation numbers $n_{\mathbf{k}}$ via $\langle a_{\mathbf{k}^*}a_{\mathbf{k}'}\rangle = n_{\mathbf{k}}\delta_{\mathbf{k}}\delta_{\mathbf{k}'}$. In equilibrium the superfluid (condensate) corresponds to $k=0$ node, with the normal fluid (thermal cloud) being distributed according to the Rayleigh–Jeans distribution

$$n_k^{eq} = \frac{k_B T}{\hbar^2k^2/2m - \mu}, \quad [14]$$

which is the classical approximation of the Bose–Einstein distribution. With the tangle of vortices the long-wavelength part of the Fourier spectrum corresponds to the superfluid (quasicondensate). The wavenumber that separates superfluid with the tangle of vortices from the normal fluid can be found from the integral distribution function $F_k = \sum_{k'\le k} n_{\mathbf{k}'}$, which exhibits a clear "shoulder" in its shape separating two regions where F_k has different slopes (54). The position of this shoulder determines the wavenumber span of the normal component. The temperature at equilibrium is defined through $n_0/(F_{k_{\max}} - n_0) = 1 - (T/T_\lambda)^{3/2}$, where $k_{\max}$ represents the maximum numerical wavenumber in the system. This expression is valid for a uniform ideal Bose gas and is an approximation for interacting superfluids.

As becomes evident from this discussion, there are at least three issues that require some refinement: (*i*) the numerical truncation of modes at the value $k_{\max}$ that makes the result dependent on the numerical resolution; (*ii*) an approximate way used to identify the temperature at equilibrium; and (*iii*) the classical distribution of thermal modes. In the next two sections we discuss the concepts and numerics that fix these problems. For simplicity of presentation the methods are formulated for the cubic NLSE (GPE). Their application to Eq. **3** then becomes straightforward.

Truncated Equations of Nonlinear Classical Fields

Microcanonical Description. Two variants of the numerical implementation of a projection (or truncation) on a finite number of Fourier modes are commonly used in the literature, known as the projected GPE (PGPE) (58) and the truncated GPE (TGPE). An equation of this form is obtained from the GPE by simply truncating the Fourier transform of the wavefunction for $|\mathbf{k}| > k_{\max}$, such that only highly occupied modes are considered. The TGPE, in the limit of cubic nonlinearity and local interaction (Eq. **5**), explicitly reads

$$i\hbar\frac{\partial\psi}{\partial t} = \mathcal{P}_G\left[-\frac{\hbar^2}{2m}\nabla^2\psi + V_0\mathcal{P}_G\left[|\psi|^2\right]\psi\right], \quad [15]$$

where we have introduced the Galerkin projector $\mathcal{P}_G$ via the Fourier space definition $\mathcal{P}_G[\hat{\psi}_{\mathbf{k}}] = \theta(k_{\max} - |\mathbf{k}|)\hat{\psi}_{\mathbf{k}}$, where $\theta(\cdot)$ is the Heaviside function. Eq. **15** exactly conserves the energy $H = \int d^3x((\hbar^2/2m)|\nabla\psi|^2 + (V_0/2)[\mathcal{P}_G|\psi|^2]^2)$ and the number of particles $N = \int d^3x|\psi|^2$. Using Fourier pseudospectral methods, the momentum $\mathbf{P} = i\hbar/2\int d^3x(\psi\nabla\overline{\psi} - \overline{\psi}\nabla\psi)$ is also conserved with dealiasing performed by the two-thirds rule [$k_{\max} = 2/3\times M/2$ at resolution M (60)]. With this procedure, in each spatial direction one-third of the available modes are not used. Instead of the

nonlinear term $\mathcal{P}_G[\mathcal{P}_G[|\psi|^2]\psi]$, the conventional PGPE formulation (55) uses the term $\mathcal{P}_G[|\psi|^2\psi]$, for which momentum conservation requires dealiasing at $k_{max} = 1/2 \times M/2$ and one-half of the available modes are lost to truncation. (Without proper dealiasing, momentum is not conserved; see appendix B of ref. 61.). Microcanonical equilibrium states are well-known to result from long-time integration of **15** and involve a condensation mechanism (55, 62, 63).

Similar classical truncated systems have been studied since the early 50s in the context of fluid mechanics. Indeed, the (conservative) Euler equation, when spectrally truncated, admits absolute equilibrium solutions with Gaussian statistics and equipartition of kinetic energy among all Fourier modes (64–67). Furthermore, the dynamics of convergence toward equilibrium involves a direct energy cascade toward small scales and contains (long-lasting) transients that mimic (irreversible) viscous effects that are produced by the "gas" of high-wavenumber partially thermalized Fourier modes generating (pseudo-)dissipative effects (68–70). In the TGPE (Eq. **15**) case, thermodynamic equilibrium can also be obtained by a direct energy cascade, in a way similar to that of the truncated Euler case, but with final thermalization accompanied by vortex annihilation. Furthermore, increasing the amount of dispersion produces a slowdown of the energy transfer at small scales, inducing a bottleneck and a partial thermalization that is independent of the truncation wavenumber (71).

Grand-Canonical Description. Grand-canonical states, allowing a direct control of the temperature (instead of the energy in the microcanonical framework), are given (61) by the probability distribution $\mathbb{P}_{st}[\psi] = \mathcal{Z}^{-1}\exp[-\beta(H - \mu N - \mathbf{v}_n \cdot \mathbf{P})]$, where $\beta = (Tk_B)^{-1}$ and the Lagrange multipliers conjugated to the number of particles and momentum are, by definition, the chemical potential μ and some velocity, chosen as the normal velocity $\mathbf{v}_n$. [The reason for this choice is that states with $\mathbf{v}_n \neq 0$ cannot, generally, correspond to a condensate moving at velocity $\mathbf{v}_s = \mathbf{v}_n$ because $\mathbf{v}_s$ is the gradient of a phase and takes discrete values for finite-size systems. In such cases the $\mathbf{v}_n$ term generates a counterflow $\mathbf{w} = \mathbf{v}_n - \mathbf{v}_s$ (61)]. Due to the quartic character of H, grand-canonical states described by $\mathbb{P}_{st}[\psi]$ are non-Gaussian. They can be efficiently obtained by constructing a nonlinear diffusion equation with noise whose stationary probability is $\mathbb{P}_{st}[\psi]$ (70). This stochastic Ginzburg–Landau equation (SGLE) is defined by the Langevin equation:

$$\hbar\frac{\partial\psi}{\partial t} = \mathcal{P}_G\left[\frac{\hbar^2}{2m}\nabla^2\psi - V_0\mathcal{P}_G\left[|\psi|^2\right]\psi\right] + \mathcal{P}_G[\mu\psi - i\hbar\mathbf{v}_n\cdot\nabla\psi] + \sqrt{\frac{2\hbar}{\mathcal{V}\beta}}\mathcal{P}_G[\zeta(\mathbf{x},t)], \qquad [16]$$

where the white noise $\zeta(\mathbf{x},t)$ satisfies $\langle\zeta(\mathbf{x},t)\zeta^*(\mathbf{x}',t')\rangle = \delta(t-t')\,\delta(\mathbf{x}-\mathbf{x}')$. The term $i\hbar\,\mathbf{v}_n\cdot\nabla\psi$ induces an asymmetry in the repartition of sound waves and generates nonzero momentum states. Equilibrium states with nonzero values of the counterflow $\mathbf{w} = \mathbf{v}_n - \mathbf{v}_s$ can be generated in this way. The SGLE (16) is not a "physical" evolution equation but is, nevertheless, of great practical use because its solutions relax to the Boltzmann probability $\mathbb{P}_{st}[\psi]$ and therefore describe thermal equilibrium. The relaxation is much faster than the TGPE microcanonical relaxation, and the direct control of the temperature of the thermalized states is also a very useful trick, for instance when dealing with phase transitions.

A somewhat similar equation, known as the stochastic (projected) Gross–Pitaevskii equation, or S(P)GPE (72–74), has been used to study properties of weakly interacting trapped atomic gases. Although dynamical equilibration with the S(P)GPE generates the correct thermal state (58, 75), the S(P)GPE can additionally describe nonequilibrium dynamics (73, 76–81). Its two closely related formulations, with or without an explicit projector (see also ref. 82 for additional "scattering" terms), and their relation to the SGLE are briefly discussed in *SI Text*.

The microcanonical and grand-canonical ensembles are known to be equivalent and thus the condensation transition reported in refs. 55, 62 is simply the standard second-order λ-transition (61) (visualized, e.g., by looking at the statistical weight of distribution $\mathbb{P}_{st}[\psi]$ with $\mathbf{v}_n = 0$).

Coupled Kinetic Equations: The Zaremba, Nikuni, and Griffin Model

An alternative microscopic formulation to such classical field methods is based on the concept of symmetry breaking, following directly from Beliaev's prescription (83), of separating the field operator $\hat{\Psi}(\mathbf{r},t) = \psi_c(\mathbf{r},t) + \hat{\psi}'(\mathbf{r},t)$, into a condensate wavefunction (ensemble average $\psi_c(\mathbf{r},t) = \langle\hat{\Psi}(\mathbf{r},t)\rangle$) and a residual fluctuating part ψ'. This explicit distinction into condensate and noncondensate components enables the derivation of two coupled equations for each subcomponent.

In the sufficiently dilute limit (no simultaneous three-body collisions), Kirkpatrick and Dorfman (84–86) formulated a coupled two-component kinetic theory by separating out the $k = 0$ mode from the excited modes of the system; this approach accounted for the Bogoliubov excitation spectrum and included a collision-based source term associated with particle transfer into or out of the condensate, and leading to damping. Motivated by recent controlled nonequilibrium studies of weakly interacting ultracold dilute atomic condensates, this approach was revisited for inhomogeneous condensates by Zaremba, Nikuni, and Griffin (87, 88), often termed the "ZNG" theory.

Dynamical equations for the condensate and noncondensate components (in direct analogy to the normal and superfluid components of the two-fluid model) are obtained from the Heisenberg equations of motion for ψ_c and ψ' treated perturbatively at the Hartree–Fock level, combined with a semiclassical description for the noncondensate via the single-particle Wigner distribution function $f(\mathbf{p},\mathbf{r},t) = \int d\mathbf{r}' e^{i\mathbf{p}\cdot\mathbf{r}'/\hbar}\langle\hat{\psi}'^{\dagger}(\mathbf{r}+\mathbf{r}'/2,t)\hat{\psi}'(\mathbf{r}-\mathbf{r}'/2,t)\rangle$. In the limit of a local pseudopotential of strength V_0—compare with Eq. **5**—one obtains the following set of coupled equations (87, 88):

$$i\hbar\frac{\partial\psi_c(\mathbf{r},t)}{\partial t} = \left\{-\frac{\hbar^2\nabla^2}{2m} + V_0\left[n_c(\mathbf{r},t) + 2n'(\mathbf{r},t)\right]\right\}\psi_c(\mathbf{r},t) - iR(\mathbf{r},t)\psi_c(\mathbf{r},t); \qquad [17]$$

$$\frac{\partial f}{\partial t} + \frac{\mathbf{p}}{m}\cdot\nabla_{\mathbf{r}}f - (\nabla_{\mathbf{r}}U)\cdot(\nabla_{\mathbf{p}}f) = C_{12}[f,\psi_c] + C_{22}[f]. \qquad [18]$$

Eq. **17** takes the form of a generalized GPE for the condensate wave function ψ_c, with $n_c = |\psi_c|^2$; this is similar to Eq. **5**, but additionally includes: (i) a mean-field potential $2V_0n'$ of the noncondensate atoms through which the condensate atoms propagate, where $n'(\mathbf{r},t) = \int(\mathbf{d^3p}/h^3)f(\mathbf{p},\mathbf{r},t)$, and ($ii$) a dissipative term $-iR\psi_c$ which allows the transfer of particles into and out of the condensate via energy- and momentum-conserving binary collisions. Self-consistency implies that the thermal atoms also propagate through an effective potential, $U = 2V_0(n_c + n')$. Eq. **18** is a quantum Boltzmann equation for the distribution function f of thermal particles; this includes both free evolution and collisional processes, and is modified from the usual Boltzmann equation form by collisional processes that allow for particles to be transferred between the condensate and the thermal cloud.

Although Eq. **17** looks similar in form to Eq. **5**, apart from the additional terms, care is needed when relating the quantity ψ_c of Eq. **17** to ψ of Eq. **5**. Whereas the latter refers to the condensate as a classical field (a multimode field in the presence of interactions), the former equation only describes the lowest-lying (self-consistent) mode directly identified as the condensate, with (thermal) excitations treated separately by the quantum Boltzmann equation (Eq. **18**). However, the explicit ZNG separation into a condensate mode and thermal excitations implies that the collisional integrals appearing in the evolution of the distribution

function f contain both stimulated (f_i) and spontaneous [$\cdots + 1$ in $(f_i + 1)$] terms; this should be contrasted with the corresponding classical-field equation which does not (implicitly) include spontaneous terms.

An appealing feature of ZNG is its applicability to two distinct regimes of quantum fluid evolution: (*i*) in the hydrodynamic regime applicable to strongly interacting liquid ^{4}He, the arising hydrodynamic equations are more general than Eqs. **9** and **10**, attaining the same structure as the Landau–Khalatnikov two-fluid equations which account for dissipation due to transport in ^{4}He (88); (*ii*) in the mean-field–dominated regime, mostly relevant for dilute trapped quantum gases, ZNG describes both collisional processes (Monte Carlo sampling) and vortex cores (no arbitrary cutoff) and reconnections fairly accurately, including the full Bose–Einstein distribution function (compare to Eq. **14**). Nonetheless, its underlying assumption of a coherent (single-mode) condensate coupled to single-particle excitations, and the absence of a stochastic kick, restricts its validity far from the critical fluctuation regime. More details about ZNG and its collision integrals C_{12} and C_{22} are given in *SI Text*.

Numerous other approaches exist for the nonequilibrium finite-temperature modeling of quantum gases, as reviewed in ref. 29: we highlight here two methods (see also *SI Text*). Firstly, we note that symmetry breaking, relied upon in ZNG, is not a requirement for a consistent coupled condensate–thermal cloud kinetic formulation, and an alternative number-conserving approach which explicitly maintains the operator part of the condensate has been constructed (see ref. 89 and references therein), relevant mainly for rather small systems of trapped atomic gases. Moreover, a convenient simplification of both the ZNG and the S(P)GPE methods leads to a dissipative GPE for the condensate, which nonetheless is capable of qualitatively reproducing nonequilibrium features and has been broadly used in the context of superfluid turbulence (9, 15, 16, 21).

Having reviewed the most common ways to deal with the thermal cloud in weakly interacting BECs, we briefly summarize some of their key predictions for the dynamics of single vortices–vortex rings, before focusing on a topical application of the proposed framework to the problem of vortex multiplication in superfluid helium.

Applications to Finite-Temperature Vortex Dynamics

Firstly we revisit the validity of the phenomenological mutual friction description of Eq. **2**, in the context of the previously analyzed models. Within the TGPE, straight vortex lines and rings in a homogeneous system were found to behave consistently with Eq. **2**. Expressing $\alpha = B\rho_n/2\rho, \alpha' = B'\rho_n/2\rho$, the weakly temperature-dependent dimensionless parameters B and B' were found to be of order unity (90) for straight vortices, and in the context of vortex rings (63). Furthermore, using the SGLE to prepare initial data with counterflow, it is known that the counterflow can block the contraction of vortex rings and also induce a dilatation (90).

The temperature dependence of α and α' was also studied in the context of a single off-centered vortex in a harmonically confined quasi-2D weakly interacting condensate (91), where the vortex deviates from its circular trajectory along the equipotential by spiraling out to regions of lower density. Throughout its decaying motion, the vortex core of the condensate is filled by thermal atoms [of approximately constant density (92)], which are believed to continuously interact with the surrounding thermal cloud. The first mutual friction contribution was found to dominate, with α increasing with both increasing temperature and atom number, whereas α' did not display a clear dependence on the parameters probed, with its small value consistent with previous results (63, 90). The related S(P)GPE study of the decay of a single vortex (80) revealed the important role of the stochastic kick for $T \approx T_c$, with persistent current decay found to be well-described (81) by such an appropriately generalized approach.

In the context of a vortex ring in a finite-temperature bath, the TGPE found a rather unexpected strong dependence of the translational velocity on the temperature, an order of magnitude above the standard transverse mutual friction effect of Eq. **2**. This can be related to the anomalous translational velocity due to finite-amplitude Kelvin waves found previously in refs. 93, 94. Assuming equipartition of the energy of the ring's thermally excited Kelvin waves with the heat bath yields a formula that gives a very good quantitative estimate of the numerically observed effect (90). Although the TGPE model is only expected to give (at best) qualitative predictions in the physical case of superfluid ^{4}He, it nonetheless naturally includes thermal fluctuations that excite Kelvin waves and these fluctuations are generic features of finite-temperature superfluids. Their strong slowdown effect on the ring translational velocity is experimentally testable.

Thus, studies of the mutual friction coefficients for the motion of a single vortex in a dilute atomic gas have revealed good agreement between the classical field method (63), the truncated equations (90), and the ZNG framework (91) (see also ref. 95 for corresponding predictions of the GPE coupled to Bogoliubov–de Gennes equations). Although such approaches have already been implemented to study various aspects of superfluid turbulence (see, e.g., refs. 54, 61, 96), this remains an exciting and rapidly growing area, with more experimental and theoretical results anticipated in the coming years.

To illustrate phenomena that can be studied in the context of these finite-temperature frameworks for the gNLSE of Eq. **3**, we now turn our attention to the particular problem of the dynamics of a vortex ring in superfluid helium.

Vortex Multiplication in Superfluid Helium

In this section we illustrate the use of the classical field methods when applied to superfluid helium. In particular, we consider the evolution of a vortex ring in the context of Eq. **7** at low and high temperatures. The equation of state of superfluid helium incorporated in Eq. **7** allows one to study the effects of negative pressure on vortices. In particular, the behavior of vortices as pressure oscillates between negative and positive values is relevant to understanding the nature of electron bubbles trapped on vortices in a set of experiments performed over the years by Maris and his colleagues (31, 32). Due to repulsive interactions with helium atoms, electrons in superfluid helium form a soft bubble of about 19 Å in radius at atmospheric pressure. The experiments are based on the property of the electron bubble to become unstable and explode at a critical pressure of about −1.89 bar. When vortices are present electrons are attracted to vortex cores due to the Bernoulli effect, with the force inversely proportional to the cube of the distance between the vortex line and the electron. This force pushes the electrons toward the vortex core until they become trapped in their cores; this process was elucidated in the context of the NLSE equation (97, 98). The flow around the trapped electron bubble acquires a circulation, therefore reducing the pressure around it. As a result, the bubbles that are trapped on vortices explode at an applied negative pressure of a smaller magnitude than that required for an electron bubble away from a vortex (31). Indeed, the experiments that measure the negative pressure required to explode an electron bubble in superfluid helium (32) show the existence of distinct thresholds in such critical pressure. Two of these were identified with electron bubbles not attached to a vortex and bubbles attached to a vortex. These two groups existed across the entire range of temperatures. However, there was another mysterious class of objects that existed for low temperature only and required even smaller in magnitude negative pressures for their explosion than the first two groups. These were referred to as "unidentified electron objects." Maris and colleagues suggested that this could be due to electrons being trapped on a doubly quantized vortex or on more than one vortex. However, it was not clear how this would be possible, as a multiply quantized vortex is dynamically unstable to breaking into singly quantized vortices, and so should not even exist. For an electron to be trapped by multiple vortices seemed highly unlikely as the trapping vortices have to be extremely close to each other and

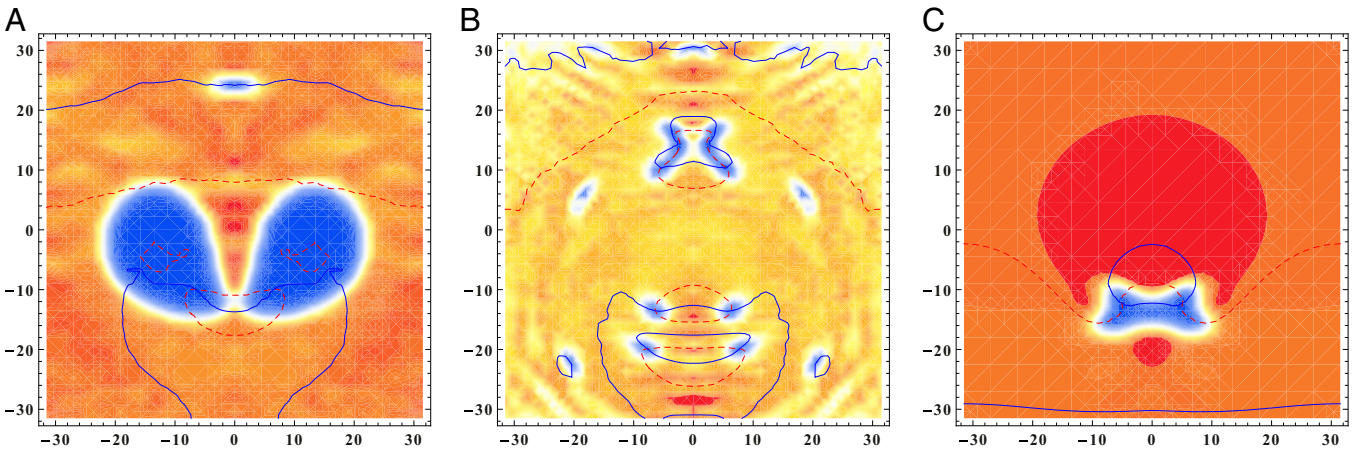

Fig. 1. Density plot of the vortex ring cross-section. Distances are in healing lengths. Vortex is moving in the positive vertical direction: (*A*) at negative pressure ($\gamma = 0.9$), (*B*) low-temperature regime; after contraction three vortex rings are generated. (*C*) High-temperature regime after contraction with a single ring remaining. Dashed and solid lines represent the zeros of real and imaginary parts, so their intersection gives the position of the vortex core and allows one to separate them from rarefaction pulses also seen on these plots as localized density depletions. The plot for high temperature is obtained after the high-frequency modes were filtered out. Such filtering was not needed for the low-temperature plots.

have the same orientation. It was not clear which processes would create such vortices.

An analog of Eq. **7** has been used in ref. 43 to study the evolution of a point vortex in varying pressure at $T = 0$. It was shown that as the pressure is lowered to negative values the vortex core enlarges as expected, but during the contraction stage at increasing pressure the vortex core "splits" into many vortices of various signs of circulation (in sum maintaining the circulation of the original vortex in agreement with the Kelvin circulation theorem). It was suggested that this mechanism explains how the electron bubble can get trapped into more than one vortex: It simply gets trapped by two or more parallel vortices during the vortex core contraction with new vortex generation. It was not clear how this would relate to 3D scenario and to high temperatures where no unidentified electron objects were detected experimentally (32).

One can envision that the scattering of vortices with the thermal cloud, the finite-amplitude sound waves, and rarefaction pulses (99–101) changes the dynamics of the vortex ring and its behavior when negative pressure is applied. To elucidate the vortex multiplication during the vortex core contraction at finite temperatures, we implemented the classical-field method using Eq. **7**, as the physics associated with the existence of the roton minimum does not seem to be relevant for this problem. In dimensionless form,

$$-2i\psi_t = \left[\nabla^2 + |\psi|^2 + \chi_4\gamma|\psi|^4 - \chi_6\gamma^2|\psi|^6 + \left(\chi_6\gamma^2 - \chi_4\gamma - 1\right)\right]\psi, \qquad [19]$$

where we rescaled the distance, $\mathbf{x} \to \xi\mathbf{x}$, by healing length $\xi = \hbar/\sqrt{2V_0 m\gamma\psi_a^2}$, time by $t \to (\xi^2 m/\hbar)t$, and the wave function by $\psi \to \sqrt{\gamma}\psi_a\psi$, with ψ_a being the uniform unperturbed state at atmospheric pressure. The dimensionless parameter γ relates the uniform state at atmospheric pressure to that at a different pressure via $\psi^2_{\text{uniform}} = \gamma\psi_a^2$. The dimensionless parameters χ_4 and χ_6 are given by $\chi_4 = V_1\psi_a^2/V_0 = 1.10337$, $\chi_6 = V_2\psi_a^4/V_0 = 1.64744$ using the known value of the superfluid uniform number density at atmospheric pressure $n_a = \psi_a^2 = 0.0218546$ Å^{-3}.

The initial state of our simulations is a vortex ring in a thermally equilibrated state. We can generate this state by numerically

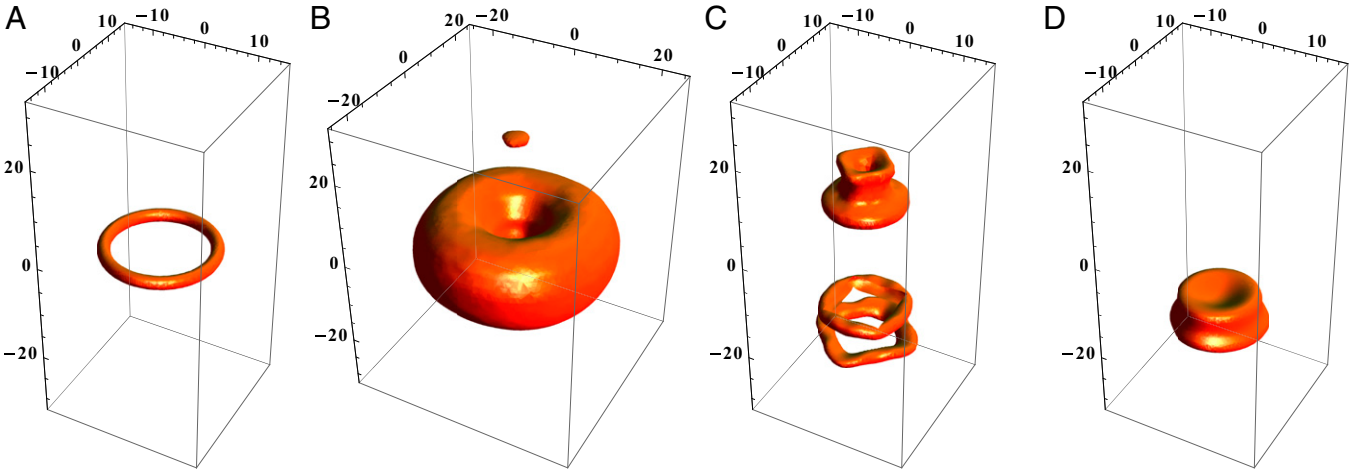

Fig. 2. Surface density time snapshots. The contour of $\rho = 0.4\rho_\infty$ is shown on each graph. (*A*) Initial state for the low-temperature simulations; (*B*) the ring after the expansion at negative pressure; (*C*) after contraction in the low-temperature regime three vortex rings are formed; (*D*) after contraction in the high-temperature regime only one vortex ring remains.

integrating Eq. **19** starting with a randomly distributed collection of harmonics, until it equilibrates, to get the condensate with a normal fluid (thermal cloud) distributed according to Eq. **14**. The initial state with the ring is the product of the thermally equilibrated state ψ_{thermal} and a wave function of the vortex ring at $T = 0$. Alternatively, one may use the SGLE (Eq. **16**) to generate a ψ_{thermal} quickly and to directly control the temperature at equilibrium.

We consider the evolution of a vortex ring in the following circumstance. The pressure in the system with a single vortex ring that is initially at zero pressure $(\gamma = 1)$ is suddenly quenched to −3.66 bar (which in our units corresponds to setting $\gamma = 0.9$) and is allowed to expand its core size (the "expansion stage"). After that the pressure is returned to zero and the subsequent evolution of the ring is recorded (the "contraction stage"). We consider this evolution at two temperatures: "low" at $T = 0.05T_\lambda$ and "high" at $T = 0.5T_\lambda$. During the expansion stage the vortex rings reduce their radii at different rates at different temperatures in accordance with $dR/dt = -\alpha u(R)$, so the high-temperature ring is reduced in its radius more dramatically than the low-temperature ring, but apart from this the processes at the two temperatures are quite similar: the vortex cores expand somewhat nonuniformly (as seen in Fig. 1*A*) due to the curvature of the vortex core. Because we are primarily interested in comparing the contracting stage between vortex rings at different temperatures, we consider this stage for two rings of the same radii. The results of the contraction stage are seen in Fig.1*B* for low temperature and Fig.1*C* for high temperature. At low temperature the vortex cores collapsed, producing three separate vortex rings of various radii rapidly moving away from each other. When this vortex formation occurs in the vicinity of an electron bubble, one may expect that the bubble is likely to be captured by more than one vortex ring. At high temperature there remains a single vortex ring rapidly reducing in size. The process of "vortex multiplication" is completely suppressed by scattering with a normal fluid component, and the probability of an electron bubble to be trapped by more than one ring is negligible. The 3D time snapshots of the vortices are given in Fig. 2. We conclude that unidentified electron objects at low temperature are electrons trapped by more than one vortex line produced during the vortex core contraction as pressure is increased. This also explains why in experiments (32) such objects were not found, as high temperature suppresses such mechanisms of vortex multiplication.

Conclusions

In the past decade much theoretical work has been done to model finite temperature in weakly interacting Bose–Einstein condensates. The starting point of such models is the cubic NLSE (GPE), which is either an accurate model of the condensate (as in ZNG formalism) or an accurate description of all highly occupied modes in a weakly interacting gas (as in classical-field models).

The requirement of weak interactions is essential for the validity of these models as it is the necessary condition for the derivation of the GPE. In a strongly interacting system, such as superfluid helium, it is impossible to divide single-particle modes into highly occupied and practically empty ones, so there are always quantum modes with occupation numbers of order unity coupled to the rest of the system. Nevertheless, as we show in this paper, it is possible to write a classical matter field equation that mathematically is analogous to the Landau two-fluid model, but also accurately accounts for the processes associated with quantized vortices.

This framework gives rise to a number of numerical issues that can be dealt with in the context of the methods that model finite temperature in weakly interacting gases, and we shortly reviewed the elements that can be used and generalized. In principle, one should allow for both features of strong phase fluctuations and dynamics of high-lying ("nonmacroscopically occupied") modes to be simultaneously accounted for; in effect, this would correspond to still enforcing a distinction into low-lying macroscopically occupied modes (as in the c-field methods), while also allowing for their coupling to the above cutoff atoms for which the full quantum Boltzmann equation (Eq. **18**) should be simulated. [The latter would automatically enforce a natural high-energy gradual cutoff in the occupation numbers due to the Bose–Einstein (as opposed to classical Rayleigh–Jeans) distribution]. A hybrid of these two methods (see, e.g., ref. 75 for related discussion) should resolve all such issues and lead to a potentially improved unified description of all stages of evolution.

The investigation of superfluid turbulence remains an active topic of research and experiments currently underway in both liquid helium and trapped weakly interacting gases, combined with continuously evolving theoretical models promise interesting developments in the years ahead. We hope that the present article will help stimulate further work in this important and still partly open area.

ACKNOWLEDGMENTS. N.P.P. acknowledges discussions with Joy Allen, Carlo Barenghi, Angela White, and Eugene Zaremba. This work was partially supported by FP7 European Union network and the Skolkovo Foundation (N.G.B.) and the UK Engineering and Physical Sciences Research Council (EPSRC) (Grant EP/IO19413/1 to N.P.P.).

1. Fetter AL (2009) Rotating trapped Bose-Einstein condensates. *Rev Mod Phys* 81(2): 647–691.
2. Barenghi CF, Donnelly RJ, Vinen WF, eds (2001) *Quantized Vortex Dynamics and Superfluid Turbulence* (Springer, Berlin).
3. Kozik EV, Svistunov BV (2009) Theory of decay of superfluid turbulence in the low-temperature limit. *J Low Temp Phys* 156(3):215–267.
4. Tsubota M, Kobayashi M, Takeuchic H (2013) Quantum hydrodynamics. *Phys Rep* 522(3):191–238.
5. Nemirovskii SK (2013) Quantum turbulence: Theoretical and numerical problems. *Phys Rep* 524(3):85–202.
6. Maurer J, Tabeling P (1998) Local investigation of superfluid turbulence. *Europhys Lett* 43(1):29–34.
7. Nore C, Abid M, Brachet ME (1997) Kolmogorov turbulence in low-temperature superflows. *Phys Rev Lett* 78(20):3896–3899.
8. Stalp SR, Skrbek L, Donnelly RJ (1999) Decay of grid turbulence in a finite channel. *Phys Rev Lett* 82(24):4831–4834.
9. Kobayashi M, Tsubota M (2005) Kolmogorov spectrum of superfluid turbulence: numerical analysis of the Gross-Pitaevskii equation with a small-scale dissipation. *Phys Rev Lett* 94(6):065302.
10. Sasa N, et al. (2011) Energy spectra of quantum turbulence: Large-scale simulation and modeling. *Phys Rev B* 84(5):054525.
11. Proment D, Nazarenko S, Onorato M (2009) Quantum turbulence cascades in the Gross-Pitaevskii model. *Phys Rev A* 80(5):051603(R).
12. Proment D, Nazarenko S, Onorato M (2012) Sustained turbulence in the three-dimensional Gross–Pitaevskii model. *Physica D* 241(3):304–314.
13. Nowak B, Sexty D, Gasenzer T (2011) Superfluid turbulence: Nonthermal fixed point in an ultracold Bose gas. *Phys Rev B* 84(2):020506(R).
14. Kraichnan RH (1967) Inertial ranges in two dimensional turbulence. *Phys Fluids* 10(7): 1417–1420.
15. Reeves MT, Anderson BP, Bradley AS (2012) Classical and quantum regimes of two-dimensional turbulence in trapped Bose-Einstein condensates. *Phys Rev A* 86(5): 053621.
16. Reeves MT, Billam TP, Anderson BP, Bradley AS (2013) Inverse energy cascade in forced two-dimensional quantum turbulence. *Phys Rev Lett* 110(10):104501.
17. Bradley DI, et al. (2006) Decay of pure quantum turbulence in superfluid 3He-B. *Phys Rev Lett* 96(3):035301.
18. Walmsley PM, Golov AI (2008) Quantum and quasiclassical types of superfluid turbulence. *Phys Rev Lett* 100(24):245301.
19. Baggaley AW, Barenghi CF, Sergeev YA (2012) Quasiclassical and ultraquantum decay of superfluid turbulence. *Phys Rev B* 85(6):060501(R).
20. Paoletti MS, Fisher ME, Sreenivasan KR, Lathrop DP (2008) Velocity statistics distinguish quantum turbulence from classical turbulence. *Phys Rev Lett* 101(15):154501.
21. White AC, Barenghi CF, Proukakis NP, Youd AJ, Wacks DH (2010) Nonclassical velocity statistics in a turbulent atomic Bose-Einstein condensate. *Phys Rev Lett* 104(7): 075301.
22. Barenghi CF, L'vov V, Roche P-E (2013) Velocity spectra of quantum turbulence: experiments, numerics and models. arXiv:1306.6248.
23. Kivotides D, Vassilicos JC, Barenghi CF, Khan MAI, Samuels DC (2001) Quantum signature of superfluid turbulence. *Phys Rev Lett* 87(27):275302.
24. Skrbek L, Sreevivasan KR (2012) Developed quantum turbulence and its decay. *Phys Fluids* 24:011301.
25. Paoletti MS, Lathrop DP (2011) Quantum turbulence. *Ann Rev Condens Matter Phys* 2(1):213–234.
26. Tsubota M, ed (2009) *Quantum Turbulence,* Progress in Low Temperature Physics (Elsevier Science, Amsterdam), Vol 16.

27. Henn EAL, Seman JA, Roati G, Magalhães KM, Bagnato VS (2009) Emergence of turbulence in an oscillating Bose-Einstein condensate. *Phys Rev Lett* 103(4):045301.
28. Wilson KE, Samson EC, Newman ZL, Neely TW, Anderson BP (2013) Experimental methods for generating two-dimensional quantum turbulence in Bose-Einstein condensates. *Ann Rev Cold Atoms Mol* 1:261–298.
29. Proukakis NP, Gardiner SA, Davis MJ, Szymanska MH, eds (2013) *Quantum Gases: Finite Temperatures and Non-equilibrium Dynamics* (Imperial College Press, London).
30. Allen AJ, Parker NG, Proukakis NP, Barenghi CF Quantum turbulence in atomic Bose-Einstein condensates. arXiv:1302.7176.
31. Classen J, Su C-K, Maris HJ (1996) Observation of exploding electron bubbles in liquid helium. *Phys Rev Lett* 77(10):2006–2008.
32. Ghosh A, Maris HJ (2005) Observation of a new type of electron bubble in superfluid helium. *Phys Rev Lett* 95(26):265301.
33. Bradley AS, Anderson BP (2012) Energy spectra of vortex distributions in two-dimensional quantum turbulence. *Phys Rev X* 2(4):041001.
34. Nowak B, Erne S, Karl M, Schole J, Sexty D, Gasenzer T (2013) Non-thermal fixed points: Universality, topology, and turbulence in Bose gasesarXiv:1302.1448.
35. Landau L (1941) Theory of the superfluidity of helium II. *Phys Rev* 60(4):356–358.
36. Vinen HE, Hall HE, Vinen WF (1956) The rotation of liquid helium II. II. The theory of mutual friction in uniformly rotating helium II. *Proc R Soc Lond A Math Phys Sci* 238(1213):215–234.
37. Bekarevich IL, Khalatnikov IM (1961) Phenomenological derivation of the equations of vortex motion in He II. *Sov Phys JETP* 13:643–646.
38. Barenghi CF, Jones CA (1987) On the stability of superfluid helium between rotating concentric cylinders. *Phys Lett A* 122(8):425–430.
39. Schwarz KW (1982) Generation of superfluid turbulence deduced from simple dynamical rules. *Phys Rev Lett* 49(4):283–285.
40. Schwarz KW (1985) Three-dimensional vortex dynamics in superfluid^4 He: Line-line and line-boundary interactions. *Phys Rev B* 31(9):5782–5804.
41. Schwarz KW (1988) Three-dimensional vortex dynamics in superfluid^4 He: Homogeneous superfluid turbulence. *Phys Rev B* 38(4):2398–2417.
42. Pitaevskii L, Stringari S (2003) *International Series of Monographs on Physics: Bose-Einstein Condensation* (Oxford Univ Press, New York), Vol 116.
43. Berloff NG (2009) Vortex splitting in subcritical nonlinear Schrödinger equations. *Fluid Dyn Res* 41(5):051403.
44. Dalfovo F (1992) Structure of vortices in helium at zero temperature. *Phys Rev B Condens Matter* 46(9):5482–5488.
45. Berloff NG (1999) Nonlocal nonlinear Schrödinger equations as models of superfluidity. *J Low Temp Phys* 116(5/6):1–22.
46. Berloff NG, Roberts PH (1999) Motions in a Bose condensate VI. Vortices in a nonlocal model. *J Phys A: Math Gen* 32(30):5611.
47. Berloff NG, Roberts PH (2000) Roton creation and vortex nucleation in superfluids. *Phys Lett A* 274(1-2):69–74.
48. Putterman SJ, Roberts PH (1983) Classical non-linear waves in dispersive nonlocal media, and the theory of superfluidity. *Phys A: Stat Mech Appl* 117(2):369–397.
49. Steel MJ, et al. (1998) Dynamical quantum noise in trapped Bose-Einstein condensates. *Phys Rev A* 58(6):4824–4835.
50. Levich E, Yakhot V (1978) The kinetics of Bose-condensation. *Ann Isr Phys Soc* 2: 861–865.
51. Kagan Yu, Svistunov BV, Shlyapnikov GV (1992) The Bose-condensation kinetics in an interacting Bose-gas. *Zh Eksp Teor Fiz* 101:528–534.
52. Kagan Yu, Svistunov BV, Shlyapnikov GV (1992) Kinetics of Bose condensation in an interacting Bose gas. *Sov Phys JETP* 74(2):279–285.
53. Kagan Yu, Svistunov BV (1997) Evolution of correlation properties and appearance of broken symmetry in the process of Bose-Einstein condensation. *Phys Rev Lett* 79(18):3331–3334.
54. Berloff NG, Svistunov BV (2002) Scenario of strongly nonequilibrated Bose-Einstein condensation. *Phys Rev A* 66(1):013603.
55. Davis MJ, Morgan SA, Burnett K (2001) Simulations of Bose fields at finite temperature. *Phys Rev Lett* 87(16):160402.
56. Góral K, Gajda M, Rzażewski K (2001) Multimode dynamics of a coupled ultracold atomic-molecular system. *Phys Rev Lett* 86(8):1397–1401.
57. Brewczyk M, Gajda M, Rzazewski K (2007) Classical fields approximation for bosons at nonzero temperatures. *J Phys B: At Mol Opt Phys* 40(2):R1–R37.
58. Blakie PB, Bradley AS, Davis MJ, Ballagh RJ, Gardiner CW (2008) Dynamics and statistical mechanics of ultra-cold Bose gases using c-field techniques. *Adv Phys* 57(5): 363–455.
59. Carruthers P, Dy KS (1966) Coherent states and irreversible processes in anharmonic crystals. *Phys Rev* 147(1):214–222.
60. Gottlieb D, Orszag SA (1977) *Numerical Analysis of Spectral Methods* (Society for Industrial and Applied Mathematics, Philadelphia).
61. Krstulovic G, Brachet ME (2011) Energy cascade with small-scale thermalization, counterflow metastability, and anomalous velocity of vortex rings in Fourier-truncated Gross-Pitaevskii equation. *Phys Rev E* 83(6):066311.
62. Connaughton C, Josserand C, Picozzi A, Pomeau Y, Rica S (2005) Condensation of classical nonlinear waves. *Phys Rev Lett* 95(26):263901.
63. Berloff NG, Youd AJ (2007) Dissipative dynamics of superfluid vortices at nonzero temperatures. *Phys Rev Lett* 99(14):145301.
64. Lee TD (1952) On some statistical properties of hydrodynamical and magneto-hydrodynamical fields. *Q Appl Math* 10(1):69–74.
65. Kraichnan R (1955) On the statistical mechanics of an adiabatically compressible fluid. *J Acoust Soc Am* 27(3):438–441.
66. Kraichnan R (1973) Helical turbulence and absolute equilibrium. *J Fluid Mech* 59: 745–752.
67. Orszag SA (1977) Statistical theory of turbulence. *Les Houches 1973: Fluid Dynamics*, eds Balian R, Peube JL (Gordon and Breach, New York).
68. Cichowlas C, Bonaïti P, Debbasch F, Brachet M (2005) Effective dissipation and turbulence in spectrally truncated Euler flows. *Phys Rev Lett* 95(26):264502.
69. Krstulovic G, Mininni PD, Brachet ME, Pouquet A (2009) Cascades, thermalization, and eddy viscosity in helical Galerkin truncated Euler flows. *Phys Rev E* 79(5):056304.
70. Krstulovic G, Cartes C, Brachet M, Tirapegui E (2009) Generation and characterization of absolute equilibrium of compressible flows. *Int J Bifurcat Chaos* 19(10): 3445–3459.
71. Krstulovic G, Brachet ME (2011) Dispersive bottleneck delaying thermalization of turbulent Bose-Einstein condensates. *Phys Rev Lett* 106(11):115303.
72. Stoof HTC (1999) Coherent versus incoherent dynamics during Bose–Einstein condensation in atomic gases. *J Low Temp Phys* 114(1-2):11–108.
73. Stoof HTC, Bijlsma MJ (2001) Dynamics of fluctuating Bose-Einstein condensates. *J Low Temp Phys* 124(3-4):431–442.
74. Gardiner CW, Davis MJ (2003) The stochastic Gross–Pitaevskii equation: II. *J Phys B: At Mol Opt* 36(23):4731.
75. Proukakis NP, Jackson B (2008) Finite temperature models of Bose–Einstein condensation. *J Phys B: At Mol Opt* 41(20):203002.
76. Proukakis NP (2003) Coherence of trapped one-dimensional (quasi-)condensates and continuous atom lasers in waveguides. *Laser Phys* 13:527–536.
77. Weiler CN, et al. (2008) Spontaneous vortices in the formation of Bose–Einstein condensates. *Nature* 455:948–951.
78. Cockburn SP, et al. (2010) Matter-wave dark solitons: Stochastic versus analytical results phys. *Phys Rev Lett* 104(17):174101.
79. Damski B, Zurek WH (2010) Soliton creation during a Bose-Einstein condensation. *Phys Rev Lett* 104(16):160404.
80. Rooney SJ, Bradley AS, Blakie PB (2010) Decay of a quantum vortex: Test of non-equilibrium theories for warm Bose-Einstein condensates. *Phys Rev A* 81(2):023630.
81. Rooney SJ, Neely TW, Anderson BP, Bradley AS (2013) Persistent current formation in a high-temperature Bose-Einstein condensate: An experimental test for c-field theory. *Phys Rev A* 88(6):063620.
82. Rooney SJ, Blakie PB, Bradley AS (2012) Stochastic projected Gross-Pitaevskii equation. *Phys Rev A* 86(5):053634.
83. Beliaev ST (1958) Application of the methods of quantum field theory to a system of bosons. *Sov Phys JETP* 7:289–299.
84. Kirkpatrick TR, Dorfman JR (1983) Transport theory for a weakly interacting condensed Bose gas. *Phys Rev A* 28(4):2576–2579.
85. Kirkpatrick TR, Dorfman JR (1985) Transport in a dilute but condensed nonideal Bose gas: Kinetic equations. *J Low Temp Phys* 58(3-4):301–333.
86. Kirkpatrick TR, Dorfman JR (1985) Time correlation functions and transport coefficients in a dilute superfluid. *J Low Temp Phys* 59(1-2):1–18.
87. Zaremba E, Nikuni T, Griffin A (1999) Dynamics of trapped Bose gases at finite temperatures. *J Low Temp Phys* 116(3-4):277–345.
88. Griffin A, Nikuni T, Zaremba E (2009) *Bose-Condensed Gases at Finite Temperatures* (Cambridge Univ Press, Cambridge, UK).
89. Billam TP, Mason P, Gardiner SA (2013) Second-order number-conserving description of nonequilibrium dynamics in finite-temperature Bose-Einstein condensates. *Phys Rev A* 87(3):033628.
90. Krstulovic G, Brachet ME (2011) Anomalous vortex-ring velocities induced by thermally excited Kelvin waves and counterflow effects in superfluids. *Phys Rev B* 83(13): 132506.
91. Jackson B, Proukakis NP, Barenghi CF, Zaremba E (2009) Finite-temperature vortex dynamics in Bose–Einstein condensates. *Phys Rev A* 79(5):053615.
92. Allen AJ, Zaremba E, Barenghi CF, Proukakis NP (2013) Observable vortex properties in finite-temperature Bose gases. *Phys Rev A* 87(1):013630.
93. Kiknadze L, Mamaladze Y (2002) The waves on the vortex ring in He II. *J Low Temp Phys* 126(1-2):321–326.
94. Barenghi CF, Hänninen R, Tsubota M (2006) Anomalous translational velocity of vortex ring with finite-amplitude Kelvin waves. *Phys Rev E* 74(4):046303.
95. Kobayashi M, Tsubota M (2006) Thermal dissipation in quantum turbulence. *Phys Rev Lett* 97(14):145301.
96. Norrie AA, Ballagh RJ, Gardiner CW (2005) Quantum turbulence in condensate collisions: An application of the classical field method. *Phys Rev Lett* 94(4):040401.
97. Berloff NG, Roberts PH (2000) Capture of an impurity by a vortex line in a Bose condensate. *Phys Rev B* 63(2):024510.
98. Berloff NG (2000) Vortex nucleation by a moving ion in a Bose condensate. *Phys Lett A* 277(4-5):240–244.
99. Berloff NG (2004) 'Interactions of vortices with rarefaction solitary waves in a condensate and their role in the decay of superfluid turbulence. *Phys Rev A* 69(5): 053601.
100. Berloff NG, Roberts PH (2004) Motions in a Bose condensate: X. New results on stability of axisymmetric solitary waves of the Gross-Pitaevskii equation. *J Phys A: Math Gen* 37(47):11333.
101. Berloff NG (2002) Evolution of rarefaction pulses into vortex rings. *Phys Rev B* 65(17): 174518.